SPECTROSCOPIC, NLO, NBO, BIOCHEMICAL INVESTIGATION OF 3-(HYDROXYMETHYL)-3-METHYL-2,6-DIPHENYLPIPERIDIN-4-ONE

A.K. PANDEY*, V.K. SINGH**, A.K. SHARMA*, S.N. TIWARI*, G. MISHRA*, R.K.S. YADAV***, V.N. MISHRA****#

*Department of Physics, "K.S. Saket" P.G. College, Ayodhya (UP), India
**Uttar Pradesh Higher Education Service Comission, Prayagraj (UP), India
***Department of Physics, S.P.M.G.D.C. Bhadohi, India
****Department of Physics, "Shree Ramswaroop" Memorial Group of Professional Studies, Lucknow (UP), India, #e-mail: vnvictorious@gmail.com

Abstract. The piperidine put deep attention to research due to their pharmacological activity and hence drug designing. The derivatives of piperidine have important activities against cancers and tumor disease. Cancer most difficult diseases in the world (WHO) which is basically considered by the uncontrolled growth of abnormal cells. In present communication structural and vibrational features of piperidine derivatives 3-(hydroxymethyl)-3-methyl-2,6-diphenylpiperidin-4-one has been computed based on theoretical quantum chemical approach. The primary aspects piperidine derivatives 3-(hydroxymethyl)-3-methyl-2,6-diphenylpiperidin-4-one structure has been calculated by using optimized geometry, spectroscopic behavior, chemical reactivity and moleculardocking analysis. The info about coupled of modes were founded in vibrational features of the molecule. The stability chemical reactivity of 3-(hydroxymethyl)-3-methyl-2,6-diphenylpiperidin-4-one were predicted by using HOMO-LUMO energy gap. The molecular electrostatic surface potential (MESP) plot utilizes overall picture of accretion of charges on separate atoms in molecule which are very useful predict the nucleophilic and electrophilic charge center. Thepharmacological importance of piperidine derivatives 3-(hydroxymethyl)-3-methyl-2,6-diphenylpiperidin-4-oneare established by calculated biological activity. The inhibition properties and chemical reactivity of piperidine derivatives 3-(hydroxymethyl)-3-methyl-2,6-diphenylpiperidin-4-one is well-known by chemical reactivity descriptors by using HOMO-LUMO energies. The inhibition potentials ofpiperidine derivatives 3-(hydroxymethyl)-3-methyl-2,6-diphenylpiperidin-4-oneestablished by calculated lipophilicity, aqueous solubility, and binding affinity. The docking of molecule has been also performed with suitable target.

Key words: Piperidin, biological activity, quantum chemical approach introduction, docking.

INTRODUCTION

In medicinal field tumor is chief worries because death increases day to day in the world [40]. The last few decades, several attempts carried out to synthesize new antitumor drug. The reappearance of tumor is major problem and the opposing things of the drugs since of toxic intolerance are specific problem treatment of cancer. In this way this research's trying to design new antitumor drug molecules having high efficiency with low side effects. The naturally occurring products as well as synthesized organic molecule shows much attention towards groundwork of new

tumor protections and therapeutic agents [27, 28]. More importantly number of compounds having potential antitumor activity [25, 36].

In this continuation computation methods are important tools which predict human pharmacokinetic properties. The difficulties for the screening of large data set compounds, adversity of valuable *in silico* absorption, distribution, metabolism, excretion (ADME) to describe depositions of pharmaceutics within model's species have been recognized. Nowadays, faster, simpler, and more cost-effective than transitional investigational procedures [7]. The piperidine derivatives has important pharmaceutical compound because piperidine derivatives have reported as important antitumor activity [25] and other biological activity.

A big number of alkaloids like piperidine are found in nature. These alkaloids have much attention due to their diverse biological activities. The derivatives of several piperidine shows pharmacological activity and play important role in the drug formation. Through synthesis number of piperidine derivatives bioactivities of this nucleus are calculated [29]. The piperidine derivatives having anesthetic activity, handling of cocaine abuse, and regulating plasma glucose as well as insulin [28]. Among the different functionalities is one of the most important ones regarding. The derivatives of piperidine show several biological activities against tubercular [2], antibacterial [10, 21], fungal, tumor [7], anticancer [24], antiviral activity [3], antimalarial activity [20], antihypertension activity [46], anticoagulant activity, antipsychotic [30], antifungal [27], anti Alzheimer's activity [47], inflammatory [6, 10, 26]. The pharmacological behavior of sulfamoyl which have pharmacological and therapeutic potential is largely linked to antibacterial action, enzyme inhibition, cancer chemotherapy, diuretic action and many additional important [45]. In case of chronic mild stress by putting pests Piperine produce antidepressant like effects [14]. Now a day quantum chemical method plays important role in field of pharmaceutical industries [30, 41, 44]. In docking process docking performed with suitable target by using molecular mechanics by suitable protein [41].

Now a day, medicinal pharmaceutical chemists are attracted to synthesize these alkaloids [35, 39] Poyamozhi *et al*. have synthesized and studied biological properties of piperidine derivatives of 1,3-dimethyl-2,6-diphenylpiperidin-4-one N(4')-cyclohexyl semicarbazone [1] and piperidine diamine derivatives. The synthesis characterization of 3-(hydroxymethyl)-3-methyl-2,6-diphenylpiperidin-4-one has been done [26]. The crystal structure of 3-(hydroxymethyl)-3-methyl-2,6-diphenylpiperidin-4-one is determined by single crystal X-ray diffraction [17]. Now a day, fast growing computational techniques provide tool to the researchers to design and characterize properties of new organic as well as inorganic molecules. The quantum chemical method has an ability to get properties of transition state of molecules. The quantum chemical method provides a new pathway to researchers to synthesize new molecular site which promotes oxidation/reduction reaction which helps us to develop more biological active compounds. In the present communication we have supported the work of Mustafa Kemal Gumus *et al*. [17] and also discussed NBO, NLO, electronic, spectroscopic, and biological docking, analysis of 3-(hydroxymethyl)-3-methyl-2,6-diphenylpiperidin-4-one by using DFT method. In

ongoing research, geometry optimization of 3-(hydroxymethyl)-3-methyl-2,6-diphenylpiperidin-4-one has been carried out by using combination of density functional theory with Lee, Yang and Parr functionals [23] (DFT/B3LYP) method and 6-311++G(d,p) as the basis set. The chemical reactivity, IR spectroscopy and excited state density functional theory (TDDFT) calculations and their nature has been carried out on 3-(hydroxymethyl)-3-methyl-2,6-diphenylpiperidin-4-one by using the same level of theory. We have also calculated the biological activity of title molecule. Swiss dock is online server which utilizes to perform docking of title molecule with anti cancerous protein. This docking provides design new drug for cancerous diseases.

MATERIALS AND METHODS

B3LYP is a hybrid form of exchange-correlation functional which combines parameterized Beck's exchange term [5] and correlation term derived by Lee, Yang and Parr. The entire calculations are performed on personal laptop by using combination of DFT/B3LYP method and 6-311++G(d,p) as the basis set. The B3LYP functional combine with parameterized Beck's exchange and correlation term suggested by Lee, Yang and Parr [5, 23]. All calculation has been performed by using combination of DFT/B3LYP method and 6-311++G(d,p) basis set which already used in previous study [35, 42]. The initial geometry of title molecule is designed on Gauss View 6.0 [9]. The geometry optimization of modeled geometry has been done on G16 software [8] without any symmetry constrain. The TDDFT calculation on title molecule is performed by using same level theory. The % contribution of molecular orbital (MO) is calculated by using Gauss Sum2.2 program package. The Gauss View 6.0 is used to plot HOMO-LUMO and MESP of title molecule. The vibrational frequencies calculation has been done on optimized geometry to ensure all stationary point at true minima and vibrational frequencies are positive. The biological activity of title molecule has been calculated by using PASS online server where we have uploaded a bioinformatics structure flow chart (SIMILI) code of optimized geometry of title molecule by using same level theory. The docking of title molecule with suitable protein has been performed by using SWISS dock online server [15, 16, 18] which includes an automated in silico molecular docking technique created on the EA Dock ESS docking algorithm.

The inhibition properties of title molecule with tumor the main target predicted by SWISS dock online server protease, the potential target protein was recovered from the RCSB protein data bank (PDB ID:) [50]. The 3D structural data of as proteins and nucleic acids, etc. are available on Protein Data Bank (PDB). The 3-D structural data available on PDB generally obtained by X-ray crystallography, NMR spectroscopy, cryo-electron microscopy, and submitted

by biologists and biochemists from everywhere the world are easily available on the Internet via the websites of its of its member organizations e.g. RCSB, PDBe, etc.

The coordinated file of targeted protein responsible for tumor and ligands are uploaded to process docking procedure. The 'accurate' parameter option for docking has been employed which is measured to be the most general for the specimen of the binding modes. After docking performs the output clusters have been found and their classified created on basis of full fitness (*FF*) score by the Swiss Dock algorithm. The more negative *FF* score more suitable for binding modes for binding between ligand and receptor. The docking pictorial graphics have been made by utilizing the UCSF Chimera program [33]. Lipophilicity (log *P*) and aqueous solubility (log *S*) are calculated by using ALOGPS 2.1 program [13, 18, 43] which is founded on the electro-topological state indices and associative neural network demonstrating [13, 43]. The log *P* and log *S* are important constraints for quantitative structure-property relationship (QSPR) studies.

RESULTS

MOLECULAR STRUCTURE

The geometry of the title molecule is optimized by using combination of DFT/B3LYP method and 6-311++G(d,p) basis set. The calculated optimized energy of title molecule is −941.9521 a.u. with C1 symmetry. The animated Gauss view structure (Fig. 1) shows that the title molecule contains two benzene rings and piperidine ring which take on a chair conformation ring. The piperidine ring shows non-planarity with other two benzene rings and form dihedral angles of 84.45 ° and 79.69 °which shows good agreement with experiment data. Animated Gauss view shows that at othro position, hydrogen is replaced by ethanol group however hydrogen of meta position is replaced by oxygen in piperidine ring. The 3-(hydroxymethyl)-3-methyl-2,6-diphenylpiperidin-4-one shows orthorhombic, Pna21 crystal structure with *a* = 17.3298 Å, *b* = 14.1856 Å, *c* = 6.5857 Å [17]. The calculated bond lengths and calculated bond angles are plotted (Fig. 2 and Fig. 3) against corresponding experimental data. The correlation factor and linear correlation equation are for bond length and bond angle are shown below:
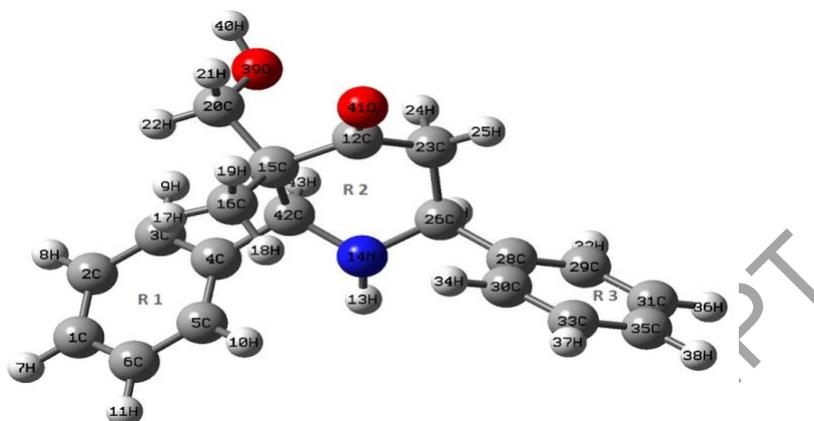
Fig. 1. Molecular structure of optimized geometry of title molecule.

$$y = 0.03391 + 0.98638x \ (R^2 = 0.98378) \text{ for bond length} \tag{1}$$

$$y = 0.95279x + 4.48728 \ (R^2 = 0.96272) \text{ for bond angle} \tag{2}$$

The calculated correlation factor shows that the calculated results well matched with experimental ones.
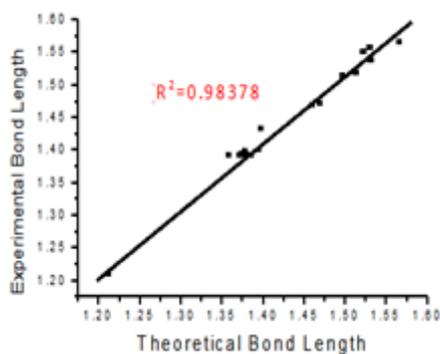

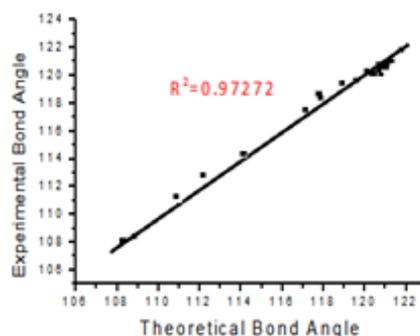Fig. 2. Theoretical bond lengths *versus* experimental bond length.

Fig. 3. Theoretical bond angles *versus* experimental bond angles.

ELECTRONIC PROPERTIES AND TDDFT CALCULATIONS

HOMO is known as highest occupied molecular orbital while LUMO as lowest unoccupied molecular orbital, also known as frontier molecular orbitals. The energy gap in between HOMO and LUMO is known as band gap [15, 16]. The chemical stability of any molecule is directly proportional to band gap in between HOMO-LUMO. A higher HOMO-LUMO gap means less polarization however less kinetic stability. The calculated HOMO-LUMO gap of title molecule shows that title molecule is less reactive in means. The HOMO-LUMO plot of title molecule is shown in Fig. 4. The HOMO of title molecule is distributed over whole molecule except ring R2 and R3 however LUMO, distributed over whole molecule. The HOMO primarily acts as donor and LUMO, as an acceptor. The transition shows that charge transfers from whole molecule to ring R2 and R3.

The MESP plot of any chemical system defines its physiochemical property relationship with molecular structure [12, 13, 22]. The intensity of electro potential surface is defined by color grading e.g., red-signify negative electrostatic potential; blue signifies the most positive electrostatic potential and green color shows zero potential. The electrostatic potential decreases as blue > green > yellow > orange > red. The MESP plot of title molecule is also shown in Fig. 5. The red color encircled over O41 however blue color encircled over N14 means O41 is most electronegative center and N14 is most electropositive charge center.
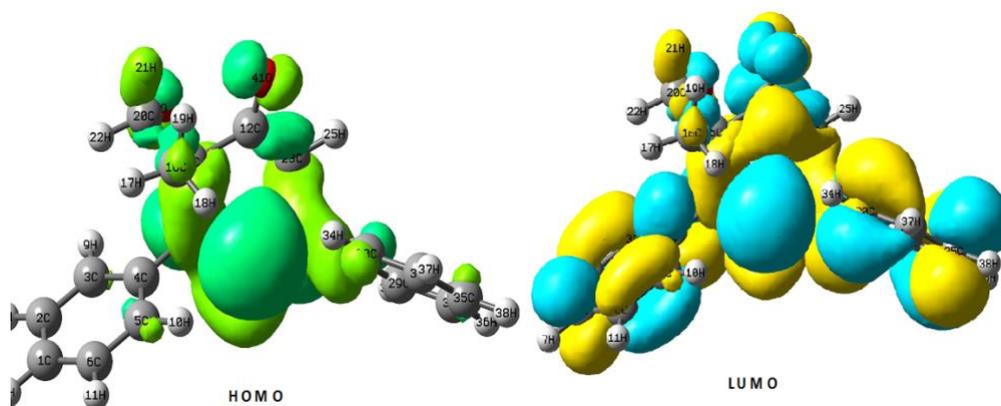
Fig. 4. HOMO-LUMO of title molecule.
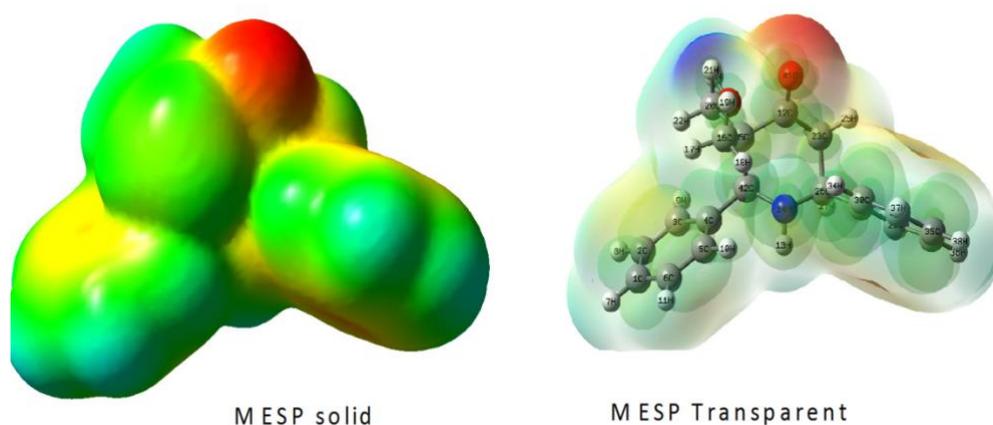
Fig. 5. MESP plots of title molecule.

Several author reports relation between HOMO-LUMO gap with hardness. The chemical hardness is directly proportional to band gap. The twice times of band gap is called chemical hardness of any molecule. The negative of eigen values of HOMO and LUMO are utilized to determine ionization potential (*IP*) and electron affinity (*EA*), respectively [32].

$$IP = -\xi_{HOMO} \text{ and } EA = -\xi_{LUMO} \tag{3}$$

where ξ_{HOMO} and ξ_{LUMO} are the eigenvalues of highest occupied molecular orbitals and lowest occupied molecular orbitals.

The chemical hardness (η) is calculated by:

$$\eta = \frac{\xi_{LUMO} - \xi_{HOMO}}{2} = \frac{IP - EA}{2} \tag{4}$$

The absolute electronegativity is calculated by using finite difference method [11, 31]. And by using energy of HOMO-LUMO, the absolute electronegativity (χ) is calculated by:

$$\chi = \frac{\xi_{LUMO} + \xi_{HOMO}}{2} = \frac{IP + EA}{2} \tag{5}$$

The chemical potential (μ) is equal to negative value of electronegativity (χ).

$$\mu = -\chi \tag{6}$$

The less band gap means molecule get more polarize and known as chemically soft molecule however reverse is true for chemically hard molecule. This explanation shows that chemical softness is just a reversal of chemical hardness [34]. The chemical softness (S) of any system is calculated by:

$$S = \frac{1}{2\eta} = \frac{1}{\xi_{LUMO} - \xi_{HOMO}} \tag{7}$$

The global electrophilicity index (ω):

$$\omega = \frac{\mu^2}{2\eta} \tag{8}$$

All global reactivity parameters of title molecule are calculated and listed in Table 1.

Table 1

Several electronic reactivity parameters of title molecule

ξ_H(eV)	ξ_L(eV)	$\xi_H - \xi_L$ (eV)	χ(eV)	μ(eV)	η(eV)	S(eV)$^{-1}$	ω
6.4721	0.8558	5.6163	3.6639	−3.6639	2.8081	0.1781	2.3902

$\xi_L = \xi_{LUMO}$; $\xi_H = \xi_{HOMO}$

TDDFT CALCULATION

The UV spectrum of title molecule is calculated by using TDDFT on optimized geometry by using same level theory. We have calculated TDDFT calculation up to twenty transition states. The calculated UV spectrum of title molecule is shown in Fig. 6. The most prominent peak appears in calculated UV spectra at 227.35 nm

which arises due to transition $S_0 \rightarrow S_9$. The calculated transition energy 5.45 eV however corresponding transition of electron occurs H-2 $\rightarrow$ LUMO (51 %), H-1 $\rightarrow$ LUMO (18 %). In this study other peaks appears at 224.33 nm with an amount of radiation absorbance between energy levels, i.e. oscillatory strength $f = 0.0292$ a.u. This peak appears due to transition of electron between $S_0 \rightarrow S_9$ which mainly due to transition of two electron H-2 $\rightarrow$ LUMO (21 %), H-1 $\rightarrow$ L+1 (20 %), H-1 $\rightarrow$ L+2 (43 %). The calculated transition energy corresponds to this peak is 5.54 eV. Some other transitions appear at 234.45 nm (having $f = 0.068$ a.u.) 219.93 nm (having $f = 0.0059$ a.u.) 215.30 nm (having $f = 0.0125$ a.u.). These peaks appear due to transition of electrons in between $S_0 \rightarrow S_7,$ $S_0 \rightarrow S_{13},$ $S_0 \rightarrow S_{18},$ respectively. The corresponding transitions energy, transitions orbitals and their % contribution are listed in Table 2.
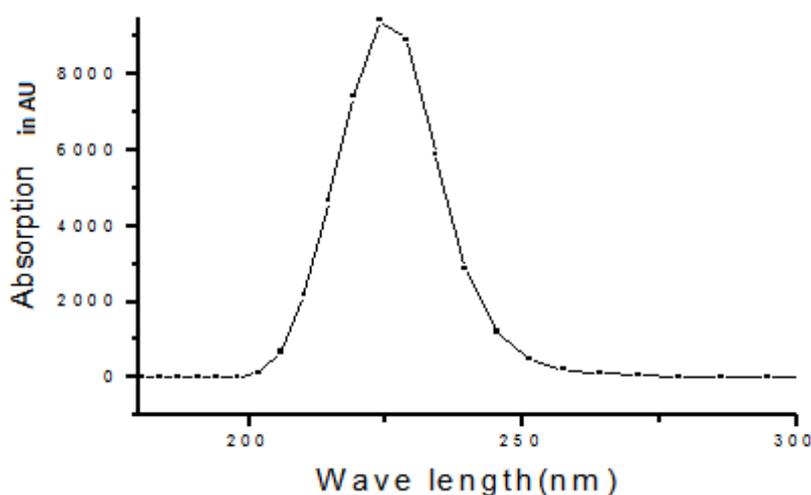
Fig. 6. Calculated UV spectrum of title molecule**.**

Table 2

The calculated values for excited state transition energy (*E),* oscillatory strength (*f*), and wavelength in TDDFT calculation

Excited state	E (eV)	f (a.u.)	Calculated λ_{max} (Å)	Transition orbitals
$S_0 \rightarrow S_8$	5.39	0.0162	230.20	H-3$\rightarrow$LUMO (12 %), H-2$\rightarrow$L+3 (11 %), HOMO$\rightarrow$L+3 (36 %)
$S_0 \rightarrow S_9$	5.45	0.0639	227.35	H-2$\rightarrow$LUMO (51 %), H-1$\rightarrow$LUMO (18 %)

$S_0 \rightarrow S_{11}$	5.53	0.0292	224.33	H-2→LUMO (21 %), H-1→L+1 (20 %), H-1→L+2 (43 %)
$S_0 \rightarrow S_{16}$	5.69	0.0143	217.76	H-4→LUMO (60 %), H-1→L+4 (−16 %)
$S_0 \rightarrow S_{18}$	5.76	0.0125	215.30	H-3→LUMO (23 %), H-3→L+4 (18 %), H-1→L+4 (14 %), H-1→L+5 (11 %)

VIBRATIONAL ANALYSIS

There are 43 atoms in title molecule consequently having 123 modes of vibration. In 123 modes of vibration, N−1 are stretching modes and rest of bending modes. The vibrations below 1000 cm^{-1} are called fingerprint region however above 1000 cm^{-1} are called functional group region. The vibrational analysis has been done on single molecule, so we have ignored molecular interactions however in this calculation we have assumed that bonds during stretching are purely elastic, so we have also ignored anharmonicity in this calculation. The calculated IR spectrum is scaled by 0.96 to compare with experimental IR spectra [38]. The calculated IR frequencies, IR intensity and assignment with % PED are listed in Table 3 only with IR intensity >10. The VEDA 4.0 program package [19] is utilized to calculate % PED of title molecule. Some important modes of vibrations are discussed below.

−OH and −NH vibrations

In present study, title molecule has –OH and −NH groups. The stretching modes of vibration of OH falls in between 3400 cm^{-1} to3600 cm^{-1} due to lower reduced mass. In present study, an intense polarized peak appears at 3699.30 cm^{-1} with PED 100 % in plane of ring R1. The in-plane OH bending appears at 1230.70 cm^{-1}, 1410.49 cm^{-1} and 1430.94 cm^{-1}; however out of plane bending modes appears at 1105.74 cm^{-1}, 216.44 cm^{-1} and 243,38 cm^{-1}. The NH stretching mode of vibration appears at 3384.08 with 99 % PED. At lower region, out plane NH bending also appears at 1087.70 cm^{-1} and 803.90 cm^{-1}.

−CH vibration

The CH stretching mode of vibration of hetero aromatic rings appears in the region from 2800 to 3100 cm^{-1}. This region is knowing as characteristics of identifying presence of –CH group [11]. In title molecule, two benzene rings are present with CH functional group. In present study, two polarized peak appears at 3057.42 cm^{-1} and 3047.34 cm^{-1} due to –CH stretching modes in aromatic benzene R1 ring however other two intense peak appears at 2861.97 cm^{-1}, and 2820.41 cm^{-1}

having PED 89 % and 94 % respectively, due to –CH stretching modes in hetero aromatic structure. At lower end of spectra in-plane bending –CH modes appears with mixing of several modes having significant intensity. In this study, in-plane bending appears at 1127.55 cm^{-1}, 1425.90 cm^{-1} and 1056.74 cm^{-1}; however, at lower region, out of plane –CH bending modes appears. The ring R2 is non planer so out of plane bending modes will appear at higher region than corresponding modes appears in aromatic benzene ring. In present study, out of plane CH bending modes are appeared at 1332.99 cm^{-1}, 1289.14 cm^{-1},1286.05 cm^{-1} and 243.16 cm^{-1}.

Methylene group / methyl group vibrations

In title molecule, both CH_3 and CH_2 groups are present at hetro aromatic ring R2. In $-CH_2/-CH_3$ group, six different modes of vibration appear with symmetric stretching, antisymmetric stretching, scissoring, rocking, wagging twisting, etc. The antisymmetric modes of vibration appear at higher frequency region than symmetric stretching modes. In present study, six back-to-back intense polarized peaks appears at 3046.23 cm^{-1}, 3057.42 cm^{-1}, 2996.78 cm^{-1},2988.60 cm^{-1}, 2933.09 cm^{-1}, and 2923.07 cm^{-1}. An intense polarized peak appears with polarized vector perpendicular to plane of ring R1 at 2884.70 cm^{-1} due to symmetric $-CH_2$ stretching. In bending modes, scissoring, and rocking modes are category of in-plane vibration however wagging and twisting modes are of out of plane bending category. The scissoring modes appear at 1450.81 cm^{-1}, 1449.02 cm^{-1}, 1425.90 cm^{-1} and 1410.49 cm^{-1}; however, rocking appears at 1221.99 cm^{-1}, 1105.74 cm^{-1} and 661.51 cm^{-1}. The wagging modes of vibration appear at 1256.05 cm^{-1}, 1230.70 cm^{-1} and 750.08 cm^{-1}.

–C=O absorption

In carbonyl group, –C=O modes of vibration are sensitive in which both carbon and oxygen are vibrating with equal amplitude. In present study an intense polarized peak appears in middle region of spectra at 1710.88 cm^{-1} with PED of 64 %.

Table 3

Calculated IR wave number, IR intensity, and their assignment by using same level theory

IR wavenumber (cm^{-1})	Intensity (a.u.)	Vibration assignment
216.44	82.7545	$\gamma\,(O_{39}H_{40})$
684.90	50.0355	$\gamma\,(CH)R_1$
690.37	32.3250	$\gamma\,(CH)R_1 + \phi_R(C_{23}H_{24}) + \phi_R(C_{23}H_{25})$
691.39	46.6479	$\phi_R(C_{23}H_{25}) + \phi_R(C_{23}H_{24}) + \gamma(C_5H_5) + \upsilon_s(C_{12}-C_{15})$
750.08	32.3942	$\phi_R(C-H)R_1$
761.13	11.3164	$\upsilon_s(C_{28}C_{30}) + \phi_w\,(N_{14}H_{13}) + \phi_R(C_{23}H_{24}) + \phi_R(C_{23}H_{25}) + \upsilon_s(C_1H_7)$
996.38	60.1317	$\upsilon_s(O_{39}C_{20}) + \phi_s(C_{16}H_{17}) + \phi_s(C_{16}H_{18})$
1006.72	15.9560	$\upsilon_s(C_{33}-C_{35})R_1 + \upsilon_s(C_{35}C_{31})R_1 + \gamma(H_{37}H_{34})R_1 + \gamma(H_{38}H_{32})R_1$
1035.61	13.7781	$\beta(C_1H_7)R_1 + \beta(C_2H_8)R_1 + \beta(C_5H_{10})R_1 + \upsilon_s(N_{14}C_{42})$
1056.74	11.4174	$\beta(C-H)R_1 + \upsilon_s(C_{35}C_{31})$
1087.70	19.4957	$\gamma(N_{14}H_{26})$
1105.74	40.8818	$\gamma(O_{39}H_{40}) + \gamma(C_{20}H_{21}) + \phi_R(C_{16}H_2) + \gamma(C_{42}H_{43})$
1121.28	65.0823	$\phi_s(C_{20}H_{22}) + \phi_w(C_{20}H_{21}) + \gamma(C_{21}H_{24}) + \upsilon_s(C_{12}C_{23})$
1171.29	12.2324	$\beta(C_{23}H_{25}) + \beta(C_{23}H_{24}) + \upsilon_s(C_{26}C_{28}) + \gamma\,(C_{33}H_{37})$
1221.99	67.3811	$\beta(C_{20}H_{21}) + \beta(O_{39}H_{40}) + \phi_R(C_{23}H_{24}) + \phi_R(C_{23}H_{25})$
1230.70	11.1186	$\beta(O_{39}H_{40}) + \beta(C_{20}H_{22}) + \phi_w(C_{23}H_2) + \gamma(N_{14}H_{13})$
1256.05	11.9321	$\gamma(C_{33}H_{37}) + \gamma(C_{30}H_{34}) + \upsilon_s(C_{30}C_{28}) + \phi_w(C_{20}H_{22}) + \phi_w(C_{20}H_{21})$
1289.14	49.6593	$\gamma(\,C_{26}H_{27}) + \gamma\,(C_{42}H_{12})$
1332.23	13.3070	$\gamma(C_{26}H_{27})R_2 + \gamma\,(C_{42}H_{43})$
1342.88	13.2011	$\upsilon_s(C_{16}C_{15}) + \phi_s(C_{16}H_3)$
1403.94	31.9527	$\phi_s(C_{23}H_{24})R_2 + \phi_s(C_{23}H_{25}) + \beta\,(O_{39}H_{40})$
1410.49	27.1550	$\phi_s(C_{23}H_{25}) + \phi_s(C_{23}H_{24}) + \beta\,(O_{39}H_{40})$
1425.90	13.4701	$\beta(CH)R_1 + \gamma(C_{30}H_{34}) + \phi_s(C_{26}H_{27}) + \phi_s(C_{26}C_{28}) + \phi_s(C_{23}H_{25}) + \phi_s(C_{23}H_{24})$
1449.02	14.9057	$\phi_s(C_{16}H_3)$ [41] $+ \phi_s(H_{22}C_{20}H_{21})$ [37]
1450.81	20.5307	$\phi_s(H_{19}C_{16}H_{18})$ [45] $+ \phi_s(H_{22}C_{20}H_{21})$ [35]
1463.37	12.6130	$\upsilon_s(C_{30}C_{28})$ [43] $+ \upsilon_s(C_{35}C_{31})$ [11] $+ \beta(H_{32}H_{36})$ [17] $+ \beta(H_{34}H_{37})$ [24]

1701.58	194.0581	$\upsilon_s(C_{12}O_{41})$ [64]
2820.41	59.3043	$\upsilon_s(C_{26}H_{27})$ [94]
2861.97	17.5079	$\upsilon_s(C_{42}H_{43})$ [89]
2884.70	39.6807	$\upsilon_s(C_{20}H_{22}H_{21})$ [93]
2923.07	22.7617	$\upsilon_{as}(C_{16}H_3)$ [97]
2933.09	23.6142	$\upsilon_{as}(C_{20}H_{22})$ [41]$+\upsilon_{as}(C_{20}H_{21})$ [54]
2988.60	16.9046	$\upsilon_{as}(C_{16}H3)$ [98]
2996.78	12.8673	$\upsilon_{as}(C_{16}H_{19})+\upsilon_{as}(C_{16}H_{18})$
3046.23	19.8806	$\upsilon_s(C_{25}H_{32})R_3+\upsilon_s(C_{30}H_{34})R_3+\upsilon_s(C_{33}H_{37})R_3+\upsilon_s$ $(C_{35}H_{38})R_3+\upsilon_s\ (C_{31}H_{36})R_3$
3047.34	16.4986	$\upsilon_s(C_5H_{10})R_1+\upsilon_s(C_6H_{11})R_1+\upsilon_s\ (C_1H_7)R_1+\upsilon_s$ $(C_2H_8)R_1+\upsilon_s(C_3H_9)R_1$
3057.42	32.1933	$\upsilon_s(C_{31}H_{36})R_1+\upsilon_s(C_{35}H_{30})R_1+\upsilon_s(C_{30}H_{34})R_1$
3057.53	17.4254	$\upsilon_s(C_5H_{10})R_1+\upsilon_s(C_1H_7)R_1+\upsilon_s(C_2H_8)R_1+\upsilon_s(C_3H_4)R_1$ $+\upsilon_s(C_{31}H_{36})R_3+\upsilon_s(C_{35}H_{38})R_3$
3384.08	12.21	$\upsilon_s(N_{14}H_{13})$ [99]
3699.31	53.6781	$\upsilon_s(O_{39}H_{40})$ [100]

Abbreviations: β = out of plane bending, γ = in plane bending, υ_s = symmetric stretching, υ_{as} = antisymmetric stretching, ϕ_s = scissoring, ϕ_R = rocking, ϕ_W = wagging.

BIOLOGICAL ACTIVITY AND DOCKING

By using ALOGPS 2.1 [13, 18, 43] the calculated values of log P and log S implies that transportation, absorption, permeability, and solubility of drug through cell membranes respectively. The calculated value of log P (−2.31) shows that the title molecule can easily transport through cell membrane. In general, value of log P lies in between −1 to −5.36. The calculated value of log S (−3.84) of title molecule lies within this range clearly indicates solubility of drugs. Where log P generally indicates the absorbance, transportability as well as distribution of any drugs in a body whereas log S signifies the water solubility of any drugs. Several biological activities of title molecule are calculated with PASS software [4]. PASS is an online server which calculate more than 900 pharmacological effects. The reliability of PASS software is judge by comparing calculated biological activities with experimentally determined biological activity of more than 46,000 drugs and after comparison accuracy of biological activity calculated by PASS is 85 %. The calculated biological activity of PASS software predicts probability to be bioactive Pa > 70 % are listed in Table 4. The Pa guesses the chance that the title molecule is fitting to the sub-class of active molecule (look like the structures of which are the most typical in a sub-set of "actives" in PASS training set). The title molecule shows good activity against nicotinic alpha6beta3beta4alpha5 receptor antagonist (0.827),

antiviral (0.783), CYP2C12 substrate (0.766), phosphatase inhibitor (0.676), etc. A nicotinic antagonist is a type of anticholinergic drug that inhibits the action of acetylcholine (ACh) at nicotinic acetylcholine receptors [49]. Title molecule will be used as anti dyskinetic drug because title molecule shows a good activity against anti dyskinetic drug. Title molecule also shows good antiviral activity so it can be used as an antiviral drug in future. Title molecule also shows good activity against gluconate 2-dehydrogenase (acceptor) inhibitor which is responsible for respiratory cancer. To design new antitumor drug, we have performed docking with suitable protein. Swiss dock is online server [36−37] which predicts and performs docking of any molecule with suitable protein. In docking process, we have uploaded mol2 file of optimized geometry of title molecule and pdb file of suitable protein. In drug discovery field interactions between a ligand and receptor leads important docking of title molecule performed blindly over whole protein not specific orientation. Swiss dock predicts that nature of gene DHODH dihydroorotate dehydrogenase (quinone) is mitochondrial [48]. The DHODH protein in tumor sequence plays an important role in mitochondrial respiratory chain in cancer cells. The pdb file of DHODH is obtained by protein data bank [50]. The calculated binding affinity, *FF* score, and H-bond, bond-length along with amino acids (residue) found in the binding site pockets are important parameters to calculate nature and strength of interaction. The binding affinity (ΔG) of (drug) compounds depends on the type of bonding (H-bond) that occurs with the active site of the protein. The docking of title molecule with DHODH protein shows two hydrogen bonds. The docking picture of title molecule with DHODH protein is shown in Figure 7. In these, binding residue of GLY-143 and GLU166 with N14 atom of title molecule are attached with bond lengths of order of 2.390 Å and 2.203 Å, respectively. The calculated force field scoring function (*FF*) and binding affinity for GLY-143 are 1123.00, −7.28 kcal/mol, respectively; however corresponding value for GLU166 are −1265.42 and −8.21 kcal/mol, respectively. The calculated force field scoring function (*FF*) and binding affinity shows that title molecule will well bind with DHODH protein as compared with some previous study.
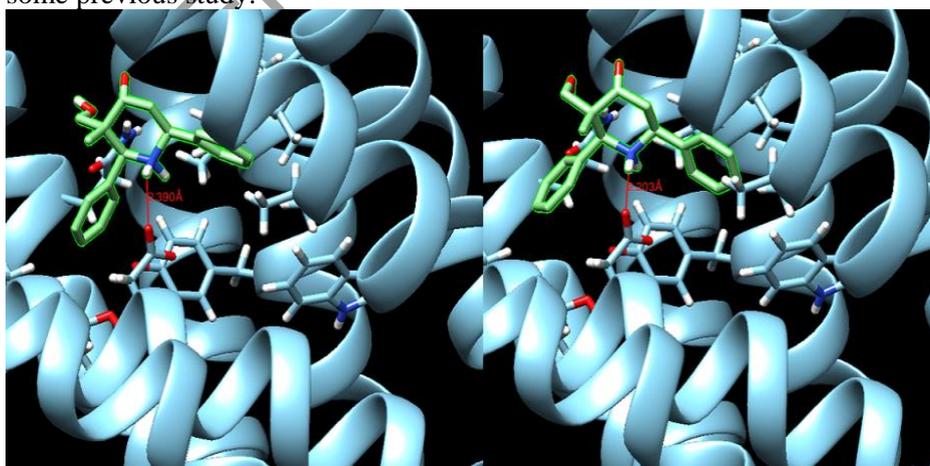
Fig. 7. Docking picture of title molecule with DHODH protein.

Table 4

Several activities calculated by PASS for *Pa* > 70 %

S.N.	Biological receptors	*Pa*	*Pi*
1	Nicotinic alpha6beta3beta4alpha5 receptor antagonist	0.827	0.007
2	Testosterone 17beta-dehydrogenase (NADP$^+$) inhibitor	0.786	0.012
3	Nicotinic alpha2beta2 receptor antagonist	0.783	0.017
4	Antiviral (Influenza)	0.766	0.044
5	Testosterone 17beta-dehydrogenase (NADP$^+$) inhibitor	0.743	0.036
6	Gluconate 2-dehydrogenase (acceptor) inhibitor	0.676	0.018
6	Antidyskinetic	0.640	0.079

Pi = the probability to be bioinactive.

CONCLUSION

In the present communication, structure of title molecule is optimized by using DFT/B3LYP and 6-311++G(d,p) as the basis set. The calculated correlation factor for bond length and bond angle shows that present method is quite well to define the geometry of title molecule. The calculated energy gap between HOMO and LUMO shows that title molecule is not chemically reactive. The TDDFT calculation shows that most intense peak appears at 227.35 nm which arises due to transition $S_0 \rightarrow S_9$. The title molecule shows good activity against nicotinic alpha6beta3beta4alpha5 receptor antagonist (0.827), antiviral (0.783), CYP2C12 substrate (0.766), phosphatase inhibitor (0.676), etc. Title molecule binds well with the cancer protein DHODH residue of GLY-143 and GLU166, so the title molecule will be uses as an anti-cancer drug in future.

Conflict of interest: The authors declare that they have no conflict of interest.

R E F E R E N C E S

1.   ANANDA, P.S., A. SETUKUMAR, C.U. KUMAR, K. KRISHNASWAMY, S. SENTHAN, G. MANIKANDAN, A. PRAKASAM, Synthesis, spectroscopic investigation, computational, stereochemical andbiological studies of 1,3-dimethyl-2,6-diphenylpiperidin-4-one *N*(4')-

cyclohexylsemicarbazone: Crystal structure and Hirshfeld surface analysis, *Chemical Data Collection.*, 2019, **21,** 100216.

2.   ARIDOSS, G., S.A. GANESAN, N.A. KUMAR, J.T. KIM, K.T. LIM, S. KABLIN, Y.T. JEONG**,** A facile synthesis, antibacterial, and antitubercular studies of some piperidin-4-one and tetrahydropyridine derivatives, *Bioorg. Med. Chem. Lett.*. 2008, **18**, 6542−6548.

3.   ARIDOSS, G., S.A. GANESAN, Y.T. JEONG, Synthesis, crystal and antibacterial studies of diversely functionalized tetrahydropyridin-4-ol, *Bioorg. Med. Chem. Lett.*, 2010, **20**, 2242−2249.

4.   BALASUBRAMANIUM, S., G. ARIDOSS, P. PARTHIBAN, C. RAMALINGAM, S. KABILAN, Synthesis and biological evaluation of novel benzimidazol/benzoxazolyl ethoxy piperidone oximes, *Biol. Pharm. Bull*., 2006, **29**, 125−130.

5.   BECKE, A.D., Density-functional thermochemistry. III. The role of exact exchange, *J. Chem. Phys*., 1993, **98**, 5648−5652.

6.   DECANDIA, M., F. FIORELLA, G. LOPOPOLO, A. CAROTTI, M.R. MROMANO, M.D. LOGRNO, S. MARTEL, P.A. CARRUPT, B.D. BELVISO, R. CALIANDRO, C. ALTOMARE. Synthesis and biological evaluation of direct thrombin inhibitors bearing 4-(piperidin-1-yl) pyridine at the P1 position with potent anticoagulant activity, *J. Med. Chem.*, 2013, **56**, ,8696−8711.

7.   ELMSELLEM, H., Y. ELOUADI, M. MOKHTARI, H. BENDAIF, H. STELI, A. AOUNITI, A.M. ALMEHDI, I. ABDEL-RAHMAN, H.S. KUSUMA, B. HAMMOUTI, A natural antioxidant and an environmentally friendly inhibitor of mild steel corrosion: A commercial oil of basil (*Ocimum basilicum* L.), *J. Chem. Technol. Metall*., 2019, **54**, 742−749.

8.   FRISCH, M.J., G.W. TRUCKS, H.B. SCHLEGEL, G.E. SCUSERIA, M.A. ROBB, J.R. CHEESEMAN, G. SCALMANI, V. BARONE, B. MENNUCCI, G.A. PETERSSON, H. NAKATSUJI, M. CARICATO, X. LI, H.P. HRATCHIAN, A.F. IZMAYLOY, J. BLOINO, G. ZHENG, J.L. SONNENBERG, M. HADA, M. EHARA, K. TOYOTA, R. FUKUDA, J. HASEGAWA, M. ISHIDA, T. NAKAJIMA, Y. HONDA, O. KITAO, H. NAKAI, T.VREVEN, J.A. MONTGOMERY, JR., J.E. PERALTA, F. OGLIARO, M. BEARPARK, J.J. HEYD, E. BROTHERS, K.N. KUDIN, V.N. STAROVEROV, R. KOBYASHI, J. NORMAND, K. RAGHAVACHARI, A. RENDELL, J.C. BURANT, S.S. IYENGER, J. TOMASI, M. COSSI, N. REGA, J.M. MILLAM, M. KLENE, J.E. KNOX, J.B. CROSS, V. BAKKEN, C. ADAMO, J. JARAMILLO, R. GOMPERTS, R.E. STRATMANN, O. YAZYEV, A.J. AUSTIN, R. CAMMI, C. POMELLI, J.W. OCHTERSKI, R.L. MARTIN, K.MOROKUMA, V.G. ZAKRZEWSKI, G.A. VOTH, P. SALVADOR, J.J. DANNENBERG, S.DAPPRICH, A.D. DANIELS, O. FARKAS, J.B. FORESMAN, J.V. ORTIZ, J.CIOSLOWSKI, D.J. FOX, *Gaussian 09*, Revision B.1, Gaussian., Wallingford, UK, 2010.

9.   FRISCH, M.J.., A.B. NELSON, A.J. HOLDER, *Gauss View.*, Pittsburgh, USA, 2005.

10.   FUNAKOSHI, T., S. CHAKI, N. KAWASHIMA, Y.SUZUKI, R. YOSHIKAWA, T. KUMAGI A. NAKAZATO, K. KAMEO, M. GOTO, S. OKUYAMA, *In vitro* and *in vivo* pharmacological profile of 5-[2-[4-(6-fluoro-1H-indole-3-yl)piperidin-1-yl]ethyl]-4-(4-fluorophenyl)thiazole-2-carboxylic acid amide (NRA0562), a novel and putative atypical antipsychotic, *Life Sci*., 2002, **7**(12), 1371–1384.

11.   GEERLINGS, P., F. DEPROFT, W. LANGENAKER, Conceptual density functional theory, *Chem. Rev*., 2003, **103**, 1793−1799.

12.   GGADRE, S.R., R.K. PATHAK, Maximal and minimal characteristics of molecular electrostatic potentials, *J. Chem. Phys.*, 1990, **93**, 1770–1774.

13.   GGADRE, S.R., I.H. SHRIVASTAVA, Shapes and sizes of molecular anions via topographical analysis of electrostatic potential, *J. Chem. Phys.*, 1991, **94**, 4384–4390.

14.   GIRGIS, A.S., Regioselective synthesis and stereochemical structure of anti-tumor active dispiro [3H-indole-3,2′-pyrrolidine-3′,3″-piperidine]-2(1H),4″-diones, *Eur. J. Med. Chem.*, 2009, **44,** 1257–1264.

15.   GROSDIDIER, A., V. ZOETE, O. MICHIELIN, SwissDock, a protein-small molecule dockingweb service based on EA Dock DSS, *Nucleic Acids Res.,* 2011, **39**, 270–277.

16.   GROSDIDIER, A., V. ZOETE, O. MICHIELIN, Fast docking using the CHARMM force field with EA Dock DSS, *J. Comput. Chem*., 2011, **32**, 2149–2159.

17.   GUMUS, M.K., S. KANSIZ, G.B. TULEMISOVA, N. DEGE, E. SAIF. Crystal structure and Hirshfeld surface analysis of 3-(hydroxymethyl)-3-methyl-2,6-diphenylpiperidin-4-one, 2022, **78**, 29−32.

18. HUUSKONEN, J.J., D.J. LIVINGSTONE, I.V. TETKO, Neural network modeling for estimation of partition coefficient based on atom-type electro topological state indices, *J. Chem. Inf. Comput. Sci.*, 2000, **40**, 947–948.

19. JAMROZ, H, *Vibrational Energy Distribution Analysis: VEDA 4 Program*, Warsaw, Poland 2004.

20. JIANG, Z., J. GU, C. WANG, S. WANG, N. LIU, Y. JIANG, W. ZHANG, C. SHENG, Design, synthesis, and antifungal activity of novel triazole derivatives containingsubstituted 1,2,3-triazole-piperidine side chains, *Eur. J. Med. Chem.*, 2014, **82**, 490–497.

21. JOGENSEN, W.L., E.M. DUFFY, Prediction of drug solubility from Monte Carlo simulations, *Bioorg. Med. Chem. Lett.* 2000, **10,** 1155–1160.

22. KÖSTER, A.M., M. LEBOUF, D.R. SALAHUB, Molecular electrostatic potentials from density functional theory, in: J.S. MURRAY, K. SEN, eds., *Molecular Electrostatic Potentials, Concepts and Applications*, Elsevier, Amsterdam, 1996, The Neatherland, pp. 105–142.

23. LEE, C., W. YANG, R.G. PARR, Development of the Colle-Salvetti correlation-energy formula into a functional of the electron density, *Phys. Rev. B.*,1988, **37**, 785–789.

24. LICHOTA, A., K. GWOZDZINSKI, Anticancer activity of natural compounds from plant and marine environment, *Int. J. Mol. Sci.* 2018, **19**(11), 3533.

25. MODA, T.L., L.G. TORRES, A.E. CARRARA, A.D. ANDRICOPULO, PK/DB: database for pharmacokinetic properties and predictive *in silico* ADME models, *Bioinformatics*, 2008, **24**, 2270–2271.

26. MOCHIZUKI, A., Y. NAKAMOTO, H. NAITO, K. UOTO, T. OHTA. Design, synthesis, and biological activity of piperidine diamine derivatives as factor Xa inhibitor, *Bioorg. Med. Chem. Lett.*, 2008, **18**, 782–787.

27. MOUSSAOUIEl, A., F.Z. JAWHARI, A.M. ALMEHDI, H. ELMSELLEM, K.F. BENBRAHIM, D. BOUSTA, A. BARI, Antibacterial, antifungal and antioxidant activity of total polyphenols of *Withania frutescens* L., *Bioorg. Chem.*, 2019, **93**, 103337.

28. NEWMAN, D.J., Natural products as leads to potential drugs: An old process or the new hope for drug discovery, *Med. Chem.*, 2008, **51**, 2589–2599.

29. NITHIYA, S., N. KARTIK, J. JAYABHARATHI, *In vitro* antioxidant activity of hindered piperidone derivatives, *Int. J. Pharm. Pharm. Sci.,* 2011, **3**(3), 254–256.

30. PANDEY, A.K., V. BABOO, V.N. MISHRA, V.K. SINGH, A. DWIVEDI, Comparative study of molecular docking, structural, electronic, vibrational spectra, and Fukui function studies of thiadiazole containing Schiff base – a complete density functional study, *Polycyclic Aromatic Compounds*, 2021, **42**, 13–39.

31. PARR, R.G., R.G. PEARSON Absolute hardness: companion parameter to absolute electronegativity *J. Am. Chem. Soc.*, 1983, **105,** 7512–7530.

32. PEARSON, R.G., Absolute electronegativity and hardness: applications to organic chemistry, *J. Org. Chem.*,1989, **54**, 1430–1440.

33. PETTERSEN, E.F., T.D. GODDARD, C.C. HUANG, G.S. COUCH, D.M. GREENBLATT, E.C. MENG, T.E. FERRIN, UCSF Chimera – a visualization system for exploratory research and analysis, *J. Comput. Chem.*, 2004, **25**, 1605–1607.

34. POPLE, J.A., H.B. SCHLEGLE, R. KRISHNAN, D.J. DEFREES, J.B. BINKELY, M.J. FRISCH, R.A. WHITESIDE, R.F. HOUT, W.J. HEHRE, Molecular orbital studies of vibrational frequencies, *Int. J. Quant. Chem.Sci.*, 1981, **15**, 269–275.

35. RAMESHKUMAR, N., A. VEENA, R ILLAVARASAN, M. ADIRAJ, P. SHANMUGAPANDIAN, S.K. SRIDHAR, Synthesis and biological activities of 2,6-diaryl-3-methyl-4-piperidone derivatives, *Biol. Pharm. Bull.*, 2003, 26, 188–193.

36. RAYAN, A., J. RAIYN, M. FALAH, Nature is the best source of anticancer drugs: Indexing natural products for their anticancer bioactivity, *PLOS ONE,* 2017, **12**(11), 1–12.

37. SANCHEZ-SANCHO, F., B. HERRANDON, Short syntheses of (S)-pipecolicacid, (R)-coniine, and (S)-coniceine using biocatalytically-generatedchiral building block, *Tetrahedron Asymmetry.* 1998, **9**(11), 1951−1965.

38. SCOTT, A.P., L. RANDOM, Harmonic vibrational frequencies: An evaluation of Hartree−Fock, Møller−Plesset, quadratic configuration interaction, density functional theory, and semiempirical scale factors, *J. Phys. Chem.*, 1996, **100**, 16502−16513.

39. SECK, R., A. GASSAMA, S. COJEAN, C. CAVE. Synthesis and antimalarial activity of 1,4-disubstituted piperidine derivatives, *Molecules*, 2020, **25**, 21–26.

40. SIEGEL, R., J. MA, Z. ZOU, A. JEMAL, Cancer statistics, *Ca-Cancer J. Clin*., 2014, **64**, 9−29.

41. SRIVASTAVA, A.K., A. KUMAR, H. SRIVASTAVA, N. MISRA The role of herbal plants in the inhibition of SARS-CoV-2 main protease: A computational approach, *Journal of the Indian Chemical Society* 2022, **99**, 1006−1040.

42. TAYLOR, P., J.H. BROWN, Muscarnic receptor agonists and antagonist, in: *Goodman and Gilman's The Pharmacological Basis of Therapeutics*, L.L. Brunton, R. Hilal-Dandan, B.C. Knollmann, eds., The McGraw-Hill Companies, Inc., 1990, pp. 166−186.

43. TETKO, I.V., V.Y. TANCHUK, T.N. KASHEVA, A.E. VILLA, Internet software for the calculation of the lipophilicity and aqueous solubility of chemical compounds, *J. Chem. Inf. Comput. Sci*., 2001, **41**, 246−260.

44. TIWARI, G., A.K. SRIVASTAVA, R. KUMAR, A. KUMAR, Quantum chemical and molecular docking studies on two potential hepatitis C virus inhibitors, *Main Group Chemistry*, 2019, **18**, 107–121.

45. WALDEMAR, G., S. GAUTHIER, R. JONES, D. WILKINSON, J. CUMMINGS, O. LOPEZ, R. ZHANG, Y. XU, Y. SUN, S. KNOX, S. RICHARDSON, J MACKELL, Effect of donepezil on emergence of apathy in mild to moderate Alzheimer's disease, *Int. J. Geriatr. Psychiatry*, 2011, **26**, 150–157.

46. WANG, G., L. CHEN, T. XIAN, Y. LIANG, X. ZHANG, Z. YANG, M. LUO, Discovery and SAR study of piperidine-based derivatives as novel influenza virus inhibitors, *Org. Biomol. Chem.*, 2014, **12**, 8048–8060.

47. XING, Y., S. ZHAO, Q. WEI, S. GONG, X. ZHAO, F.ZHOU, R. AI-LAMKI, D. ORTMANN, M. DU, R. PEDERSEN, G. SHANG, S. SI, N.W. MORRELL, J. YANG, A novel piperidine identified by stem cell-based screening attenuates pulmonary arterial hypertension by regulating BMP2 and PTGS2 levels, *Eur. Respir. J*., 2018, **51**(4), 17022−17029.

48. ZHOU, Y., L. TAO, X. ZHOU, Z. ZUO, L.E. TAO, X.I. ZHOU, Z.E. ZUO, J. GONG, X. LIU, Y. ZHOU, C. LIU, N. SANG, H. LIU, J. ZOU, K. GOU, X. YANG, Y. ZHAO, DHODH and cancer: promising prospects to be explored, *Cancer& Metabolism*, 2021, **9**, 1–25.

49. ***.https://www.cancer.org/content/dam/CRC/PDF/Public/8418.00.pdf

50. ***Crystal structure of human dihydroorotate dehydrogenase (DHODH) with amino-benzoic acid inhibitor 641 at 2.05A resolution, https://www.rcsb.org/structure/3kvk.